



## UvA-DARE (Digital Academic Repository)

### Structured doping of upconversion nanosystems for biological applications

Wang, Y.

**Publication date**  
2011

[Link to publication](#)

#### **Citation for published version (APA):**

Wang, Y. (2011). *Structured doping of upconversion nanosystems for biological applications*. [Thesis, fully internal, Universiteit van Amsterdam].

#### **General rights**

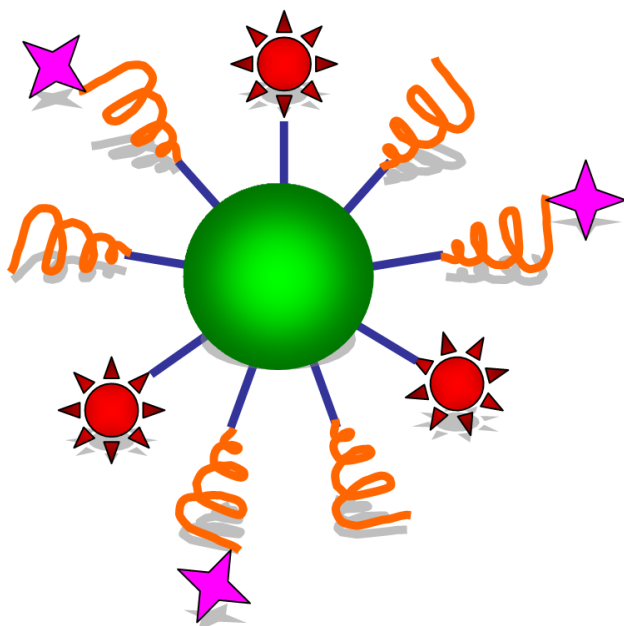
It is not permitted to download or to forward/distribute the text or part of it without the consent of the author(s) and/or copyright holder(s), other than for strictly personal, individual use, unless the work is under an open content license (like Creative Commons).

#### **Disclaimer/Complaints regulations**

If you believe that digital publication of certain material infringes any of your rights or (privacy) interests, please let the Library know, stating your reasons. In case of a legitimate complaint, the Library will make the material inaccessible and/or remove it from the website. Please Ask the Library: <https://uba.uva.nl/en/contact>, or a letter to: Library of the University of Amsterdam, Secretariat, P.O. Box 19185, 1000 GD Amsterdam, The Netherlands. You will be contacted as soon as possible.

# CHAPTER 5

## Covalently-linked Multifunctional Upconversion Nanoconjugates for Photodynamic Therapy and Imaging of Cancer Cells



## Chapter 5

**Abstract:** By covalently binding NaYF<sub>4</sub>:Yb<sup>3+</sup>,Er<sup>3+</sup> nanoparticles (UCNPs) with the photosensitizer rose bengal (RB) and folic acid (FA), an upconversion nanoparticle platform for detection and treatment of tumors has been created. Compared to the more popular approach of electrostatic interaction, the present covalent approach makes the platform more rigid and resistant to the biological environment. Upon 980 nm CW irradiation, multicolor upconverted emission is generated by the UCNPs. The 650 nm emission is used for imaging the location of the particles while 540 nm upconverted emission serves to excite RB and generate singlet oxygen for photodynamic therapy. From the confocal images of JAR choriocarcinoma cells we have confirmed the target transfection of UCNPs mediated by the FA receptor. The present system thus has the potential to serve as a new platform for integrated photodynamic diagnosis and therapy, and for real-time reporting of therapeutic efficacy during treatment.

**Keywords:** upconversion · photosensitizer · nanoconjugates · photodynamic therapy  
· imaging · covalently-link

## 5.1 Introduction

Recently, the development of rare earth ions doped upconversion nanoparticles (UCNPs) capable of converting NIR photons to visible ones has attracted considerable interest in both *in vitro* [1] and *in vivo* [2] biomedical applications. Compared to traditional fluorescent labels (such as organic dyes and quantum dots), UCNPs have the advantage that they can be excited by NIR photons. As a result, auto-fluorescence is for all practical purposes absent, while scattering of the excitation light is significantly reduced. NaYF<sub>4</sub>:Yb<sup>3+</sup>,Er<sup>3+</sup> is one of the most efficient upconversion materials with two strong upconverted emission bands around 540 nm and 650 nm.

One of the applications which may greatly benefit from the unique properties of the UCNPs is photodynamic therapy (PDT). [3] PDT is an effective, non-invasive economical treatment for cancers. PDT involves excitation of a photosensitizer molecule into an electronically excited state, which subsequently undergoes intersystem crossing to a triplet state, and then transfers the energy to ground state oxygen (<sup>3</sup>O<sub>2</sub>) to initiate the generation of cytotoxic species, such as singlet oxygen (<sup>1</sup>O<sub>2</sub>) and other reactive oxygen species (ROS). These cytotoxic species will oxidize biomolecules which leads to eventual cell death by apoptosis. The use of UCNPs for PDT was first reported in studies in 2007 when NaYF<sub>4</sub>:Yb<sup>3+</sup>,Er<sup>3+</sup> nanoparticles were coated with a thin layer of SiO<sub>2</sub> doped with Merocyanine-540 photosensitizer and functionalized with a tumor targeting antibody on the surface. [4] Under 980 nm excitation, cancer cell destruction was observed *in vitro*. This nanoplatform could be delivered highly specifically to cancer cells and was capable of killing cancer cells with low photosensitizer loading. In 2008 Y. Zhang *et al.* made 50 nm PEI/NaYF<sub>4</sub>:Yb<sup>3+</sup>,Er<sup>3+</sup> nanoparticles modified with a zinc phthalocyanin photosensitizer and targeted to folate receptors on human colon cancer cells. [3b] Significant cell destruction was observed. In 2009, this group coated NaYF<sub>4</sub> UCNPs with a uniform layer of mesoporous silica. [3c] As a result, a high loading of zinc phthalocyanine photosensitizers incorporated into the mesoporous silica could be obtained. Nevertheless, the photosensitizer ZnPc was still noncovalently adsorbed onto the nanoparticles' surface.

In the present study we introduce the use of covalently linked UCNP-RB nanoconjugates for PDT of cancer cells. Under the excitation of near infrared light, UCNP-RB conjugates emit two main bands in the visible part of the spectrum. The 540 nm emission is used for the excitation of RB for PDT, while the 650 nm emission is used for detection of the labeled cells.

## 5.2 Experiments

### 5.2.1 Chemicals

(CF<sub>3</sub>COO)<sub>3</sub>Y·3H<sub>2</sub>O, (CF<sub>3</sub>COO)<sub>3</sub>Yb·3H<sub>2</sub>O and (CF<sub>3</sub>COO)<sub>3</sub>Er·3H<sub>2</sub>O were

## Chapter 5

purchased from *GFS Chemicals*.  $\text{CF}_3\text{COONa}$ , oleylamine (OM), rose bengal (RB), 6-bromohexanoic acid, 2-aminoethyl dihydrogenphosphate (AEP), dimethylsulfoxide (DMSO), folic acid, deuterium dioxide  $\text{D}_2\text{O}$ , N-hydroxysuccinimide (NHS), 1-ethyl-3-(3-dimethylaminopropyl) carbodiimide (EDC) were purchased from *Aldrich*. 1,3-diphenylisobenzofuran (DPBF) was purchased from *Fluka*. PEG was purchased from *NANOCs*. Folic acid and RPMI 1640 medium (folate free) were purchased from *Invitrogen*.

### **5.2.2 Synthesis of $\text{NaYF}_4:\text{Yb}^{3+},\text{Er}^{3+}$ upconversion nanoparticles**

In our construction, hexagonal-phase  $\text{NaYF}_4:\text{Yb}^{3+},\text{Er}^{3+}$  UCNP was adopted because of its high upconversion efficiency compared with the cubic one. It was synthesized by thermal decomposition of trifluoroacetate precursors in oleylamine according to previously published methods.<sup>[5]</sup> In detail,  $\text{CF}_3\text{COONa}$  (2 mmol),  $(\text{CF}_3\text{COO})_3\text{Y}\cdot 3\text{H}_2\text{O}$  (0.78 mmol),  $(\text{CF}_3\text{COO})_3\text{Yb}\cdot 3\text{H}_2\text{O}$  (0.2 mmol), and  $(\text{CF}_3\text{COO})_3\text{Er}\cdot 3\text{H}_2\text{O}$  (0.02 mmol) were dissolved in oleylamine (12 mL). The mixture was heated to 120 °C to remove water and oxygen with vigorously magnetic stirring under argon flow protection for 1 hour. The mixture was then heated to 320 °C in the presence of argon for protection from oxidation. After 1 hour, the heating was stopped and the yellowish reaction mixture was allowed to cool to 80 °C. The nanoparticles were precipitated using ethanol and isolated via centrifugation for at least three times, and stored in chloroform before further treatment.

### **5.2.3 Phase transfer of upconversion nanoparticles from hydrophobic to hydrophilic**

The oleylamine terminated  $\text{NaYF}_4:\text{Yb}^{3+},\text{Er}^{3+}$  upconversion nanoparticles are hydrophobic. However, for the clinical application only hydrophilic nanoparticles can be used. Following our previous approach with slight modifications,<sup>[6]</sup> a ligand exchange process was carried out to transfer hydrophobic upconversion nanoparticles into hydrophilic ones using 2-aminoethyl dihydrogenphosphate (AEP) as ligand. 200 mg of AEP was dispersed in a 10 mL mixture of water and ethanol (volume ratio is 3:2). The hydrophobic UCNPs solution (~20 mg, purified and dispersed in 5 mL of chloroform) were mixed with the AEP solution and stirred vigorously over 48 hours at 30 °C. The UCNPs were transferred from the bottom chloroform layer to the top  $\text{H}_2\text{O}/\text{CH}_3\text{CH}_2\text{OH}$  layer. The  $\text{H}_2\text{O}/\text{CH}_3\text{CH}_2\text{OH}$  layer was then collected and washed three times by water. After centrifugation, the obtained nanoparticles were redispersed in water. After phase transfer, the AEP terminated UCNPs offer an amino group which can be used for covalently coupling with carboxyl terminated molecules.

### **5.2.4 Conjugation of upconversion nanoparticles and rose bengal photosensitizer**

First, the RB-NHS ester was synthesized as a previous protocol.<sup>[7]</sup> Then, a 2.5 mg/mL solution of  $\text{NaYF}_4:\text{Yb}^{3+},\text{Er}^{3+}$  was mixed with RB-NHS ester at room temperature for 4 hours. UCNP-RB conjugates were dialyzed in water for two days to remove

unreacted photosensitizer. Different numbers of RB molecules were conjugated to UCNPs by changing the molar stoichiometry of photosensitizer to UCNPs in the range of 10-400. All samples were stored in the dark at 4 °C after the reaction and purification procedures.

### 5.2.5 Construction of upconversion nanoconjugates: $\text{NaYF}_4:\text{Yb}^{3+},\text{Er}^{3+}$ -rose Bengal/PEG-folic acid

First, the folic acid N-hydroxysuccinimidyl ester (FA-NHS) was prepared according to the literature.<sup>[8]</sup> Then, 45 mg of FA-NHS was mixed with 100 mg of bi-functional  $\text{NH}_2$ -PEG-COOH (molar ratio 1:3) in 10 mL water and stirred for 24 hours in the dark. The resulting solution was added to 100 mg UCNP-RB solution, and reacted at room temperature for 48 hours. The nanoconjugates were collected by centrifugation and washed with water for three times. Finally, the nanoconjugates were redispersed in 10 mL phosphate buffer and stored in the dark at 4 °C. The procedure of constructing UCNP-RB/PEG-FA nanoconjugates is schematically shown in **Figure 5.1**.

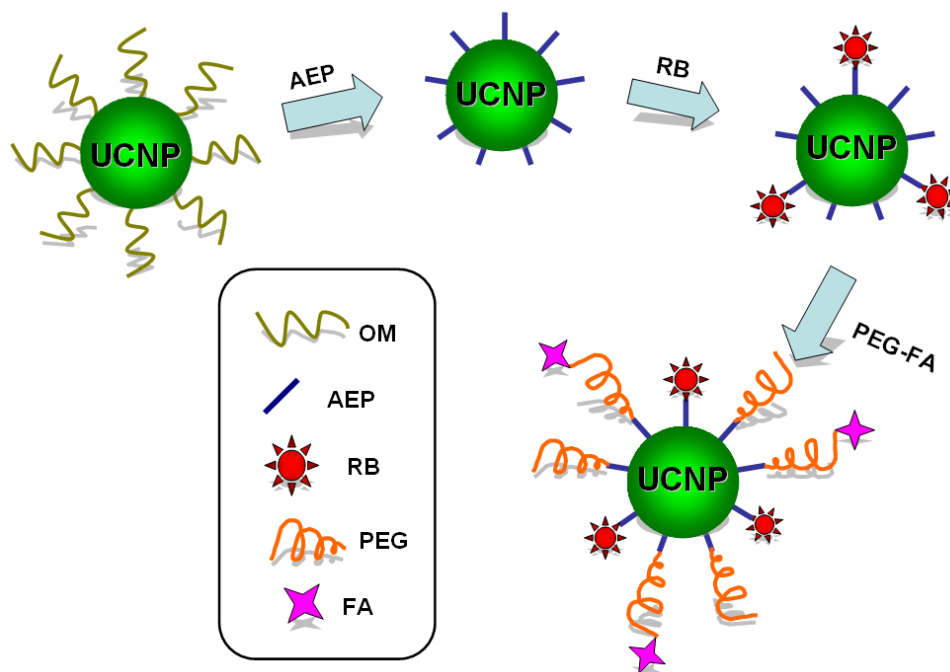


**Figure 5.1.** Schematic illustration of the construction of UCNP-RB/PEG-FA conjugates.

### 5.2.6 Upconversion luminescent spectra measurement

A Horiba Jobin Yvon Spex Fluorolog 3 spectrofluorometer system was used to detect the upconversion emission spectra. For excitation a 980 nm CW diode laser was

## Chapter 5

employed.

### **5.2.7 Singlet oxygen detection**

Generation of  $^1\text{O}_2$  by UCNP-based photosensitizers was detected chemically using the disodium salt of 1,3-diphenylisobenzofuran (DPBF) as  $^1\text{O}_2$  sensor.<sup>[9]</sup> When singlet oxygen is generated, DPBF converts to its endoperoxide form, which in turn leads to its photobleaching, which can be monitored by measuring the reduction in absorption intensity at 410 nm. In our experiments, the absorption reduction was followed as a function of time after irradiating samples with a 980 nm diode laser using a Hewlett-Packard/Agilent 8453 Diode-Array Biochemical Analysis UV-Vis Spectrophotometer. In order to detect the singlet oxygen phosphorescence emission at 1270 nm, a liquid nitrogen cooled DSS-IGA020L InGaAs detector was coupled to the system.

### **5.2.8 Cell imaging**

The JAR choriocarcinoma cell line was purchased from ATCC and cultured as follows. JAR cells were cultured in RPMI-1640 folate free medium (Gibco®, Invitrogen) supplemented with fetal bovine serum to a final concentration of 10% (Gibco®, Invitrogen), 100 U/mL penicillin, 100  $\mu\text{g}/\text{mL}$  streptomycin, maintained at 37 °C in a humidified 95% air and 5% carbon dioxide  $\text{CO}_2$  atmosphere.

### **5.2.9 Upconversion luminescence imaging of cancer cells**

JAR cells were put on the coverslip and cultured in folic acid free RPMI 1640 medium for 24 hours. Then  $\text{NaYF}_4:\text{Yb}^{3+},\text{Er}^{3+}$  nanoconjugates were added into the culture medium and incubated in physiological conditions for 6 hours. Finally, the coverslip was washed by flushing with PBS for three times in order to remove non-bonded nanoconjugates.

Wide field imaging and upconversion luminescent confocal imaging of the cancer cells was carried out using an inverted Olympus IX71 microscope system equipped with a 100 $\times$  oil immersion objective. In this setup excitation light is provided by a Chameleon ULTRA-II Ti:Sapphire laser (976 nm, 80 fs, 80 MHz, Coherent) coupled into the adapted confocal unit via a polarization maintaining single-mode fiber. A single-photon avalanche diode (TimeHarp 200, PicoQuant) is connected to the PCI-board to perform time-correlated single photon counting.<sup>[10]</sup> The emitted light passes through an 80/20 beam splitter and is sent to a SPAD and a spectrograph (Spectra Pro-150, Acton Research Corp.) equipped with a CCD camera.

### **5.2.10 MTT assay**

JAR cells were collected, diluted to a density of  $1 \times 10^5$  cells/mL in a culture medium, and seeded onto 96-well plates (100  $\mu\text{L}/\text{well}$ ). After 24 hours  $\text{NaYF}_4\text{-RB/PEG}$

nanoconjugates were added to the wells in different concentrations (25, 50, 100, 200, 500, 1000  $\mu\text{g}/\text{mL}$ ) with 5 wells for each sample, and then incubated for another 24 hours at 37 °C. The cells were washed twice with phosphate-buffered saline to remove free nanoparticles and exposed for 5 minutes to 980 nm NIR laser irradiation ( $1.0 \text{ W}/\text{cm}^2$ ). The cells were then incubated at 37 °C for an additional 48 hours, after which their viability was measured by a 3-(4,5-dimethylthiazol-2-yl)-2,5-diphenyl tetrazolium bromide (MTT) assay. The MTT assay is a colorimetric method for measuring the activity of enzymes that reduces MTT to formazan dyes which show a purple color. The cell viability and proliferation can then be calculated from the formazan absorption intensity at 550 nm. 10  $\mu\text{L}$  of MTT solution (5 mg/mL MTT in phosphate buffer solution, pH 7.4) was added to each well, after which the cells were incubated for another 2 hours at 37 °C. After removing the medium, the wells were washed in PBS and intracellular formazan crystals were extracted into 100  $\mu\text{L}$  of DMSO. They were quantified by measuring the absorbance of the cell lysate at 550 nm. All results were averages  $\pm\text{SD}$  of five samples.

### 5.3 Results and discussion

In this work, phase transfer to hydrophilic nanoparticles was conducted using AEP to replace OM on the surface of  $\text{NaYF}_4$ . The average size of the resulting hydrophilic nanoparticles was about 20 nm as shown by the TEM image in **Figure 5.2 (A)**. Amino groups ( $-\text{NH}_2$ ) can help to disperse the UCNPs stably in water, DMSO and cell culture medium.

Covalent conjugation of  $-\text{NH}_2$  and  $-\text{COOH}$  was used for coupling UCNPs and biofunctional molecules. Firstly, photosensitizer RB was covalently bound to the UCNP. After washing with water for 3 times, the colloidal nanoconjugates were redispersed in aqueous buffer and stored in the dark at 4 °C. The absorption spectrum of RB (black line) is shown in **Figure 5.2 (B)**. It overlaps perfectly with the 540 nm upconversion emission band of UCNP and thus guarantees an efficient energy transfer from UCNP to RB. To test the stability of UCNP-RB covalent conjugates, control experiments were conducted for RB adsorbed on  $\text{NaYF}_4$  via electrostatic interaction. Both samples were washed 3 times by DMSO after which the absorption spectra of eluents were recorded. Contrary to the distinct colorful elutes of the adsorption sample, the elutes from the covalently bound UCNP-RB sample remained colorless, indicating no significant dissociation of RB from the UCNP surface. We can thus conclude that these covalently bonded UCNP-RB conjugates are significantly more stable than those formed via electrostatic interaction.

Following this strategy, we were able to link other biofunctional molecules such as PEG and folic acid (FA) onto the same nanoparticles as well. For this a special PEG with dual function groups ( $\text{NH}_2\text{-PEG-COOH}$ ) was adopted as the linker to combine the nanoparticle with the targeting molecule FA, as shown in **Figure 5.1**. FA was chosen to be targeting molecule as most epithelial cancer cells overexpress folate receptor on the cell

## Chapter 5

membrane. In the present case, FA was located at the terminus of PEG to decrease the steric hindrance, which guaranteed the target efficacy for the active reception by cancer cell.

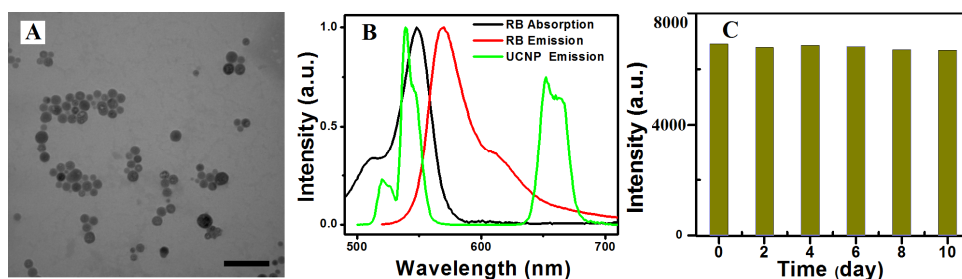


**Figure 5.2.** (A) TEM image of amino groups functionalized NaYF<sub>4</sub> nanoparticles after phase transfer, average size 20 nm; (scale bar=100 nm) (B) Green curve: upconversion emission spectrum of UCNP; black curve: RB absorption, red curve is emission spectrum of RB upon excitation of 540 nm; (C) Stability of UCNP-RB nanoconjugates in DMPI 1640 (1 mg/mL) as analyzed by spectrophotometry;

The stability of the nanoconjugates dispersed in DMPI 1640 cell culture medium was studied by monitoring the upconversion luminescence at 650 nm every 48 hours (Figure 5.2 C). The nanoparticle concentration was set at 1000  $\mu\text{g/mL}$ . Within the 10 days of research, the fluorescence intensity of UCNP-RB showed no significant reduction indicating that the nanoconjugates had good stability and dispersibility in medium, and are suitable for cell experiments.

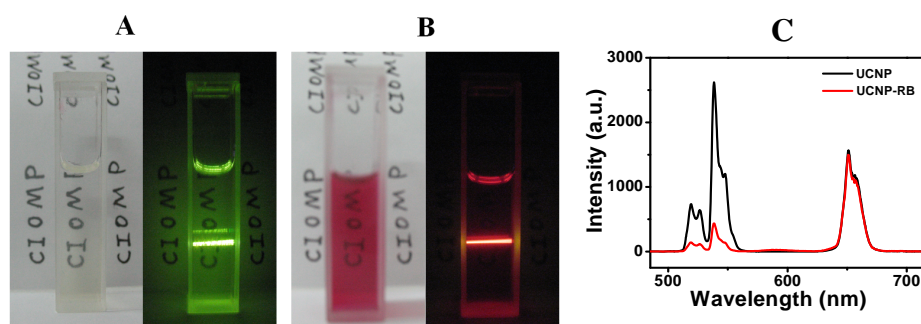


**Figure 5.3.** (A) Photographs of UCNPs under ambient light (left) and 980 nm laser diode excitation (right); (B) Photographs of UCNP - RB under ambient light (left) and 980 nm laser diode excitation (right); (C): Upconversion luminescence spectrum of the bare UCNP sample (black line) and of the UCNP-RB sample (red line).

In most cases Förster Resonance Energy Transfer (FRET) is a dipole-dipole interaction, and the spectral overlap between donor emission and acceptor absorption is crucial for an efficient FRET. As mentioned above, the 540 nm upconversion emission band overlaps well with RB absorption. Therefore, if the nanoconjugate is well constructed, excitation with 980 nm irradiation should lead to quenching of the 540 nm emission while the 650 nm emission intensity should remain unchanged. **Figure 5.3** shows that this is indeed what is observed.

Rose bengal (RB) is one of the most efficient photosensitizers, but excitation of 540 nm impedes its clinical use as this wavelength has limited tissue penetration. The UCNP-RB conjugate avoids this limitation. Using UCNP as an energy donor, RB can produce singlet oxygen under 980 nm irradiation. The release of  $^1\text{O}_2$  can be monitored by detecting its phosphorescent emission at 1270 nm.<sup>[11]</sup>

Before the experiment, the nanoconjugates were centrifuged and redispersed in  $\text{D}_2\text{O}$  at a concentration of 2 mg/mL and saturated with oxygen gas for 30 minutes. Relevant data of singlet oxygen generation are given in **Figure 5.4 A**. It is clear that the covalent modification process does not affect the optical properties of RB seriously, and that singlet oxygen can be generated efficiently via upconversion luminescent energy transfer. Generation of singlet oxygen was confirmed by the chemical probe DPBF by detection of the decay of its absorption peak at 410 nm<sup>[12]</sup> (**Figure 5.4 B**).

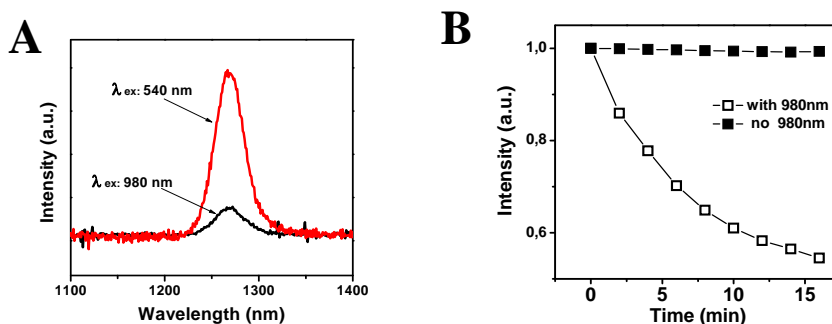


**Figure 5.4.** (A) 1270 nm phosphorescent emission of singlet oxygen ( $^1\text{O}_2$ ) produced by nanoconjugates in  $\text{D}_2\text{O}$ . Red line: excitation of RB at 540 nm, black line: excitation of nanoconjugates at 980 nm. (B) The decay curves of DPBF absorption at 410 nm caused by UCNP-RB conjugates as a function of irradiation time. The excitation wavelength is 980 nm.

Many epithelial carcinoma cells overexpress folate receptors on the membrane, which thus can be used as a target for selective drug delivery. The human choriocarcinoma cell line (JAR) is one of these cell lines, which was chosen here as an *in vitro* model. Before imaging, the live cells were washed with PBS for three times to remove excess

## Chapter 5

UCNPs in the medium, and then fixated with 90% glycerin. The top row of **Figure 5.5** displays UCNPs positive transfected JAR cells under bright field illumination (**Figure 5.5 A**). The upconversion confocal image excited with a 980 nm pulsed laser is shown in **Figure 5.5 B**. Finally, the merged bright field and upconversion image is displayed in **Figure 5.5 C**. It is clear that UCNPs are mainly located in the cytoplasmic and perinuclear regions, confirming the endocytosis of multifunctional NaYF<sub>4</sub>-RB/PEG-FA nanoconjugates. . As a contrast, **Figure 5.5 D–F** shows images of cells when a folic acid (2 mg/L) supplemented medium was adopted for cell culture in order to block the floater receptor on the membrane. Because the folate receptors are now saturated by free folic acid, only few nanoconjugates can be linked with the cell, as shown in **Figure 5.5 E** where the 650 nm upconversion intensity is distinctly reduced. The non-zero background reflects the nonspecific adsorption of UCNPs. What is equally important to notice is that there are no cell morphology changes under both conditions (**Figure 5.5 A** and **Figure 5.5 D**), which indicates the excellent biocompatibility of nanoconjugates.

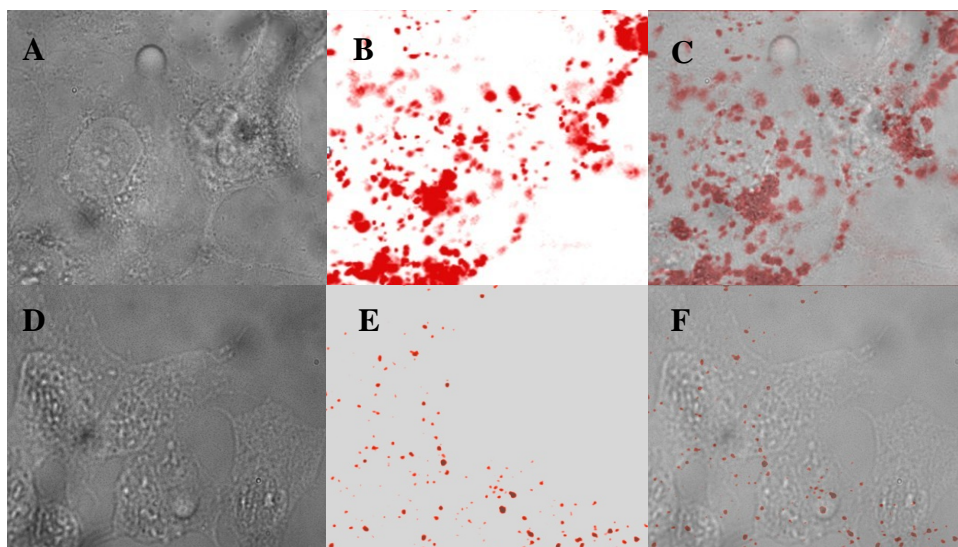


**Figure 5.5.** Bright field image (A, D) and upconversion luminescent confocal microscopy (B, E) images of JAR cells after incubation with 200  $\mu\text{g}/\text{mL}$  UCNP-RB/PEG-FA conjugates for 6 hours at 37 °C and washing three times with PBS buffer. Images C and F are the merged images of A and B, and of D and E, respectively. (A-C): Cells cultured in a folate-free medium, the positive staining shows folic acid mediated endocytosis of nanoconjugates; (D-F): Cells cultured in a folic acid supplemented medium (2 mg/L), the negative staining originates from nonspecific adsorption of nanoconjugates.

**Figure 5.6** shows the viability of cells grown for 24 hours with the nanoconjugates

with varying concentrations ranging from 2  $\mu\text{g/mL}$  to 1  $\text{mg/mL}$ . The results show that the toxicity of nanoconjugates is not so severe below a concentration of 0.5  $\text{mg/mL}$ , which is higher than the concentration usually used in cell imaging. When 980 nm light is added, more cells are killed.

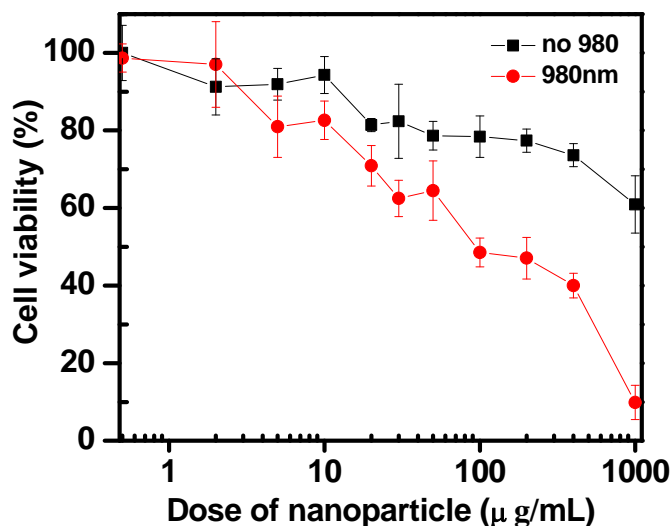


**Figure 5.6.** Cell viability of JAR cells treated with different amount of UCNP-RB conjugates. The data indicated with red circles have been obtained under 980 nm irradiation, the data indicated with black squares without radiation.

## 5.4 Conclusions

In conclusion, multifunctional upconversion nanoconjugates  $\text{NaYF}_4\text{-RB/PEG-FA}$  have been designed for target imaging and therapy of cancer cells. The covalent combination of nanoparticle, photosensitizer, and target vector has ensured that the nanoconjugates remain stable during delivery. The two upconversion emission bands located at 650 nm and 540 nm have been used for imaging and PDT, respectively. It has been demonstrated that the photosensitizer can be excited by NIR photons, which in turn leads to the generation of singlet oxygen, killing the cancer cells. Through confocal imaging using the 650 nm upconversion luminescence, the folic acid mediated endocytosis of the nanoconjugates has been demonstrated.

## 5.5 Acknowledgments

This work was supported by NSFC of China (60771051, 60601015, 10674132,

## Chapter 5

10874179, and 20603035), and the joint research program between CAS of China and KNAW of the Netherlands.

## 5.6 References

---

- 1 (a) Guidelines for Topical Photodynamic Therapy: Update. C.A. Morton, K.E. McKenna, and L.E. Rhodes; *British Journal of Dermatology*, **2008**, *159*, 1245–1266; (b) Versatile photodynamic therapy at infrared excitation. P. Zhang, P. Steelant, M. Kumar, and M. Scholfield; *J. Am. Chem. Soc.*, **2007**, *129*, 4526–4527; (c) Upconversion Fluorescence Imaging of Cells and Small Animals Using Lanthanide Doped Nanocrystals. D.K. Chatterjee, A.J. Rufaihah, and Y. Zhang; *Biomaterials*, **2008**, *29*, 937–943; (d) Synthesis, Characterization, and In Vivo Targeted Imaging of Amine-Functionalized Rare-Earth Upconverting Nanophosphors. L.Q. Xiong, Z.G. Chen, M.X. Yu, F.Y. Li, C. Liu, and C.H. Huang; *Biomaterials*, **2009**, *30*, 5592–5600; (e) Immunolabeling and NIR-Excited Fluorescent Imaging of HeLa Cells by Using NaYF<sub>4</sub>:Yb,Er Upconversion Nanoparticles. M. Wang, C.C. Mi, W.X. Wang, C.H. Liu, Y.F. Wu, Z.R. Xu, C.B. Mao, and S.K. Xu; *ACS Nano*, **2009**, *3*, 1580–1586. (f) Multicolor Core/Shell-Structured Upconversion Fluorescent Nanoparticles. Z.Q. Li, Y. Zhang, and S. Jiang; *Advanced Materials*, **2008**, *20*, 4765–4769.
- 2 (a) Highly-Sensitive Multiplexed in vivo Imaging Using PEGylated Upconversion Nanoparticles. L. Cheng, K. Yang, S. Zhang, M. Shao, S. Lee, and Z. Liu; *Nano Res.*, **2010**, *3*, 722–732; (b) High Contrast Upconversion Luminescence Targeted Imaging in Vivo Using Peptide-Labeled Nanophosphors. L.Q. Xiong, Z.G. Chen, Q.W. Tian, T.Y. Cao, C.J. Xu, and F.Y. Li; *Anal. Chem.*, **2009**, *81*, 8687–8694;
- 3 (a) Versatile Photosensitizers for Photodynamic Therapy at Infrared Excitation. P. Zhang, W. Steelant, M. Kumar, and M. Scholfield; *J. Am. Chem. Soc.*, **2007**, *129*, 4526–4527; (b) Upconverting Nanoparticles as Nanotransducers for Photodynamic Therapy in Cancer Cells. D.K. Chatterjee and Y. Zhang; *Nanomedicine*, **2008**, *3*, 73–82. (c) Mesoporous-Silica-Coated Up-Conversion Fluorescent Nanoparticles for Photodynamic Therapy. H.S. Qian, H.C. Guo, P.C.L. Ho, R. Mahendran, and Y. Zhang; *Small*, **2009**, *5*, 2285–2290; (d) Singlet Oxygen-Induced Apoptosis of Cancer Cells Using Upconversion Fluorescent Nanoparticles as a Carrier of Photosensitizer. H.C. Guo, H.S. Qian, N.M. Idris, and Y. Zhang; *Nanomedicine: Nanotechnology, Biology, and Medicine*, **2010**, *6*, 486–495.
- 4 Versatile photosensitizers for photodynamic therapy at infrared excitation. P. Zhang, W. Steelant, M. Kumar, and M. Scholfield; *J. Am. Chem. Soc.*, **2007**, *129*, 4526–4527.
- 5 (a) Synthesis of Colloidal Upconverting NaYF<sub>4</sub> Nanocrystals Doped with Er<sup>3+</sup>, Yb<sup>3+</sup> and Tm<sup>3+</sup>, Yb<sup>3+</sup> via Thermal Decomposition of Lanthanide Trifluoroacetate Precursors. J.C. Boyer, F. Vetrone, L.A. Cuccia, and J.A. Capobianco; *J. Am. Chem. Soc.*, **2006**,

- 
- 128, 7444-7445; (b) Synthesis of Hexagonal-Phase NaYF<sub>4</sub>:Yb,Er and NaYF<sub>4</sub>:Yb,Tm Nanocrystals with Efficient Up-Conversion Fluorescence. G.S. Yi, G.M. Chow; *Adv. Funct. Mater.*, **2006**, *16*, 2324-2329; (c) Upconversion Luminescence of  $\beta$ -NaYF<sub>4</sub>: Yb<sup>3+</sup>, Er<sup>3+</sup>@ $\beta$ -NaYF<sub>4</sub> Core/Shell Nanoparticles: Excitation Power Density and Surface Dependence. Y. Wang, L.P. Tu, J.W. Zhao, Y.J. Sun, X.G. Kong, and H. Zhang; *J. Phys. Chem. C*, **2009**, *113*, 7164–7169.
- 6 Hexanedioic Acid Mediated Surface–Ligand-Exchange Process for Transferring NaYF<sub>4</sub>:Yb/Er (or Yb/Tm) Up-converting Nanoparticles from Hydrophobic to Hydrophilic. Q.B. Zhang, K. Song, J.W. Zhao, X.G. Kong, Y.J. Sun, X.M. Liu, Y.L. Zhang, Q.H. Zeng, and H. Zhang; *J. Colloid. Interface. Sci.*, **2009**, *336*, 171–175.
- 7 Light-Induced Proteolysis of Myosin Heavy Chain by Rose Bengal-Conjugated Antibody Complexes. K.A. Conlon, M. Berrios; *Journal of Photochemistry and Photobiology B: Biology*, **2001**, *65*, 22-28.
- 8 Targeted Folic Acid-PEG Nanoparticles for Noninvasive Imaging of Folate Receptor by MRI. T.J. Chen, T.H. Cheng, Y.C. Hung, K.T. Lin, G.C. Liu, and Y.M. Wang; *J Biomed Mater Res A*, **2008**, *87*, 165-75
- 9 Fluorescence probes used for detection of reactive oxygen species. A. Gomes, E. Fernandes, and J.L.F.C. Lima; *J. Biochem. Biophys. Methods*, **2005**, *65*, 45–80
- 10 Polymer Glass Transitions Switch Electron Transfer in Individual Molecules. J.R. Siekierzycka, C. Hippius, F. Wrthner, R.M. Williams, and A.M. Brouwer; *J. Am. Chem. Soc.*, **2010**, *132*, 1240–1242
- 11 Quenching of Singlet Molecular Oxygen by Carnosine and Related Antioxidants. Monitoring 1270-nm Phosphorescence in Aqueous Media. S.Y. Egorov, E.G. Kurella, A.A. Boldyrev, and A.A. Krasnovsky Jr.; *Biochem Mol Biol Int.*, **1997**, *47*, 687-694
- 12 (a) Singlet Oxygen Quantum Yields of Different Photosensitizers in Polar Solvents and Micellar Solutions. W. Spiller, H. Kliesch, D. Wohrele, S. Hackbarth, B. Roder, and G.J. Schnurpfeil; *J. Porphyrins Phthalocyanines*, **1998**, *2*, 145-158; (b) Methylene Blue-Containing Silica-Coated Magnetic Particles: A Potential Magnetic Carrier for Photodynamic Therapy. D.B. Tada, L.L.R. Vono, E.L. Duarte, R. Itri, P.K. Kiyohara, M.S. Baptista, and L.M. Rossi; *Langmuir*, **2007**, *23*, 8194-8199.